PCCP

RSC Publishing

PAPER

View Article Online
View Journal | View Issue

Cite this: *Phys. Chem. Chem. Phys.*, 2013, **15**, 9308

Ultra-slow dynamics in low density amorphous ice revealed by deuteron NMR: indication of a glass transition

Florian Löw,*[a] Katrin Amann-Winkel,[b] Thomas Loerting,[b] Franz Fujara[a] and Burkhard Geil[c]

Received 23rd February 2013,
Accepted 11th April 2013

DOI: 10.1039/c3cp50818h

www.rsc.org/pccp

The postulated glass–liquid transition of low density amorphous ice (LDA) is investigated with deuteron NMR stimulated echo experiments. Such experiments give access to ultra-slow reorientations of water molecules on time scales expected for structural relaxation of glass formers close to the glass–liquid transition temperature. An involved data analysis is necessary to account for signal contributions originating from a gradual crystallization to cubic ice. Even if some ambiguities remain, our findings support the view that pressure amorphized LDA ices are of glassy nature and undergo a glass–liquid transition before crystallization.

1 Introduction

In recent years it became more and more evident that thermal as well as dynamic properties of the disordered low temperature states of water strongly depend on the history of the sample and especially on the pathways taken in a p*VT*-diagram during the preparation of the phases. The original distinction between two (high- and low density) amorphous ices (HDA and LDA) introduced by Mishima *et al.*[1] nowadays seems to be a rough classification scheme only, where we know many (re)producible variations within both classes. In the first place it is not the variability in physical properties itself that is surprising. All simple glass formers have inherited the physical properties of the liquid at the 'fictitious temperature' where the molecular kinetics of the liquid was 'frozen in' and thus their properties vary depending on the thermal sample history.

Most amorphous ices, however, do not directly stem from a frozen liquid state but are produced by a pressure-induced collapse of crystalline ice structures. Are they nevertheless related to a well-defined, higher temperature equilibrium liquid state?[2–8] Or are they the crushed, disordered, and fully out-of-equilibrium remains of a crystal structure?[9–13] If they are glasses, which of those many amorphous variations are the possibly frozen-in liquid states? Considering LDL and HDL as liquid analogs to LDA and HDA is obviously already established in the literature.[14,15] But then, do we – maybe – have a broad spectrum of LDLs and HDLs? On the other hand, if they are 'undefined' remains of a microscopically destroyed crystal, do they relax into a structure that is equivalent to a liquid that really exists at higher temperatures? Obviously, all of them seem to relax into some well-defined predefined direction. The central question is whether or not there is experimental evidence of a glass–liquid transition prior to (or hidden by) the HDA-to-LDA or the LDA-to-ice I_c transition.

During the last decade it was realized that a certain member of the LDA class of amorphous ices, previously called 'LDA-II',† exhibits a significantly extended range of thermal stability.[6,17] In LDA-II the onset of crystallization into cubic ice I_c is shifted by as much as 10 K up to higher temperatures when compared to other unrelaxed species of the LDA class. For LDA being a glass, a temperature interval of 10 K – close to the calorimetric T_g[6,18] – would imply a tremendous gain in accessible time scales for the α-relaxation. Could the gain of these 10 K on

[a] *Institut für Festkörperphysik, Technische Universität Darmstadt, Hochschulstr. 6, 64289 Darmstadt, Germany. E-mail: florian.loew@physik.tu-darmstadt.de*
[b] *Institute of Physical Chemistry, University of Innsbruck, Innrain 52a, A-6020 Innsbruck, Austria*
[c] *Institut für Physikalische Chemie, Georg–August–Universität Göttingen, Tammanstr. 6, 37077 Göttingen, Germany*

† Nelmes *et al.*[16] demonstrated that the state of relaxation of high density amorphous ice affects its properties quite significantly and therefore emphasized the necessity to distinguish between the original[1] unrelaxed or unannealed form of HDA (uHDA) and the one which is relaxed/annealed close to the transition to LDA (so called expanded HDA, eHDA). Recently, it became clear that the degree of relaxation of HDA influences the thermal stability and the intermediate range structural ordering of LDA forms, being called LDA-I (obtained from uHDA) and LDA-II (obtained from eHDA).[6,17]

the low temperature border of the so-called 'no-man's land' in the phase diagram of amorphous ices yield the key to access the liquid side of the glass-liquid transition? If not, could we at least observe the glass typical divergence of structural relaxation times? Or, in the worst case, could we, maybe, see some indications of it?

This study is not the first attempt to enter the new 10 K extension of temperature range of the no man's land's border using the stability of LDA-II. In previous work, we analyzed the new candidates eHDA and its derivative LDA-II in terms of quasielastic neutron scattering[19] and deuteron (^{2}H) NMR spin-relaxation[20] thereby looking for anomalies in the Debye–Waller factor and nuclear spin–lattice relaxation enhancement, respectively, which might then be attributed to fast glass-typical secondary processes. Our findings did not provide a clear-cut message pro or contra a glass–liquid transition.

Now, with this work, we will try to track the structural relaxation itself, utilizing ^{2}H-NMR which is able to access the ultra-slow reorientation dynamics that has to be associated with any structure relaxation in all ice-like water-networks due to the Bernal–Fowler ice rules. ^{2}H-NMR offers two complementary anchor points to study dynamic processes: spin–lattice relaxation is 'easy' to measure but 'hard' to interpret without *ad hoc* model assumptions while stimulated echoes are much 'harder' to measure but offer an 'easy' and, even more important, an unambiguous, model-free interpretation. We will use a combination of both techniques that has proven to be a powerful tool for investigations of the glass–liquid transition in many simple glass former model systems in the past.[21,22]

Fig. 1 shows the essential findings of those studies: above the caloric glass–liquid transition temperature T_g of molecular glass formers one observes the so-called α-process characterized by the structural relaxation time τ_α. The experimental spin–lattice relaxation times T_1 display a minimum at that temperature where the time constant of the relevant motional process equals the inverse Larmor frequency. As long as T_1 stems from the α-process it should follow the temperature dependence of $T_{1,\alpha}$. From relaxation theory it is known that at temperatures below the T_1 minimum (the so-called slow motion regime) $T_{1,\alpha} = C\tau_\alpha$ with $C \approx 10^4 \ldots 10^5$ for typical ^{2}H quadrupolar coupling constants and Larmor frequencies of around 40 to 50 MHz.[23] Experimentally, however, close to T_g the T_1 relaxation tends to be dominated by fast secondary processes. This results in a temperature dependence of T_1 being weaker than that of $T_{1,\alpha}$ such that close to T_g τ_α eventually crosses T_1. Below T_g the T_1 relaxation behavior is determined by dynamic properties of the amorphous structure such as phonon-like excitations or librations with decreasing amplitudes as temperature is decreased.

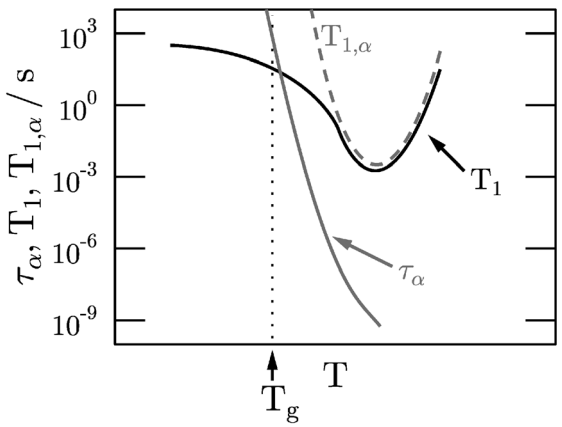

Fig. 1 Sketch of *T*-dependent ^{2}H-NMR times T_1 and structural relaxation times τ_α (solid curves) as typically measured in molecular glass formers around T_g. Above T_g, τ_α scales with viscosity η according to $\tau_\alpha(T) \propto \eta(T)/T$. As long as spin–lattice relaxation is governed by the α-process only, it is given by $T_{1,\alpha}(T)$ (dashed curve).

2 Experimental

2.1 Deuteron NMR

The NMR experiments are performed at a ^{2}H Larmor frequency of 46.7 MHz. Strong rf pulses (with π/2 pulse lengths of about 2.0 μs) have been applied to ensure full excitation of the broad deuteron powder spectra.

^{2}H-NMR is an excellent tool for observing O–^{2}H bond reorientations, since the orientation-dependent frequency shift ω_Q is dominated by the quadrupole interaction of the deuteron:

$$\omega_Q = \frac{\delta}{2}\left(3\cos^2\theta - 1 - \eta\sin^2\theta\cos 2\phi\right) \quad (1)$$

where θ is the angle between the O–^{2}H bond and the external magnetic field, $\delta = \frac{3}{4}e^2qQ/h$ is related to the quadrupole coupling constant $e^2qQ/h = (218.6 \pm 1.0)$ kHz for O–^{2}H bonds in LDA-I.[24] ‡

Magnetization recovery curves $M(t)$ are measured by application of a saturation pulse sequence with variable waiting time. The obtained recovery curve is parameterized by a stretched-exponential function (Kohlrausch law):

$$M(t) = M_0\left(1 - \exp\left[-\left(\frac{t}{T_1}\right)^\beta\right]\right). \quad (2)$$

with the time constant T_1 and the stretching parameter β.

Using the ^{2}H stimulated echo experiment "$(\pi/2) - \tau - (\pi/2) - t_m - (\pi/2) - \tau -$ echo" we can directly measure a single particle reorientation correlation function of a tagged O–^{2}H bond orientation relative to the external magnetic field direction and therefore obtain information about geometry and the time scale of the bond reorientational motion. The echo amplitude $S(\tau, t_m)$ correlates the quadrupole frequency of a tagged deuteron during the dephasing period of length τ with its quadrupole frequency during the rephasing period of length τ after mixing time t_m. For $\tau \ll t_m$ the amplitude is[25–27]

$$S(\tau, t_m) = S_0\langle e^{-i\omega_Q(0)\tau}e^{i\omega_Q(t_m)\tau}\rangle \quad (3)$$

‡ The anisotropy parameter of the electric field gradient $\eta = 0.102 \pm 0.006$ (ref. 24) is negligible in our context.

The brackets $\langle\ \rangle$ denote the ensemble average. The experimental data are parameterized by a stretched-exponential decay towards a plateau value, *i.e.*,

$$S(\tau, t_m) \propto (1 - S_\infty(\tau)) \exp\left[-\left(\frac{t_m}{\tau_c(\tau)}\right)^{\gamma(\tau)}\right] + S_\infty(\tau) \qquad (4)$$

The τ-dependent parameters are the time constant $\tau_c(\tau)$, the Kohlrausch parameter $\gamma(\tau)$ and the long time plateau value $S_\infty(\tau)$.

The amplitude of the stimulated echo experiment is not only reduced by correlation loss but also due to spin–lattice relaxation. This additional decay has to be considered as pointed out in ref. 28.

2.2 Sample preparation

The samples are prepared from ^2H_2O (99.9% deuteration) purchased from *eurisotop*. The preparation technique is described in detail by Winkel *et al.*[29] In short: LDA-II is obtained after isothermal compression of ice I_h at 110 K followed by heating to 160 K at a pressure of 1.1 GPa. Very high density amorphous ice (VHDA), obtained in this way, is subsequently decompressed isothermally at 143 K with a rate of 13 MPa min^{-1} to 8 MPa towards LDA-II. The decompression is followed by quenching to 77 K. The sample preparation has been identical to that in ref. 17, 19 and 20. X-ray powder diffractograms confirm the low density amorphous nature of all samples. Care has been taken not to exceed 85 K when transferring them into the flow cryostat of an NMR spectrometer. The temperature stability is estimated to be ±0.5 K over several days.

3 Results and discussion

In previous works, deuteron T_1 was established as a sensitive monitor parameter to verify the thermal limits of stability of various ice phases.[20,30,31] One central outcome of all those experiments was the finding that most LDA species show a slow annealing towards a common state when the temperature is cycled inside the stability range of these phases. As far as one can conclude from NMR experiments alone, the common state could be identical with LDA-II – a hypothesis that is supported by the fact that LDA-II itself shows no annealing in the whole range of its extended thermal stability.

3.1 Characterization of the sample states with T_1

In the present work, stimulated echo experiments are used to obtain temperature dependent α-relaxation times of LDA-II. For each temperature point the stimulated echo experiment is embedded within two T_1 measurements. This time consuming procedure is necessary to verify the sample stability, a precondition for the data interpretation that follows.

Fig. 2 demonstrates the quality of data underlying these control experiments. Fig. 2a shows a magnetization recovery after a saturation pulse sequence together with two least-square fit results. The dashed line, which corresponds to the residue plot shown in Fig. 2b, is obtained by fitting the data with a simple mono-exponential recovery function. Systematic deviations much stronger than the scatter in the data lead to the conclusion that the T_1 decay is not mono-exponential. Using a stretched exponential fitting function instead (the solid line and the residue plot in Fig. 2c) results in a parametrization that is flexible enough to modulate the recovery curves.

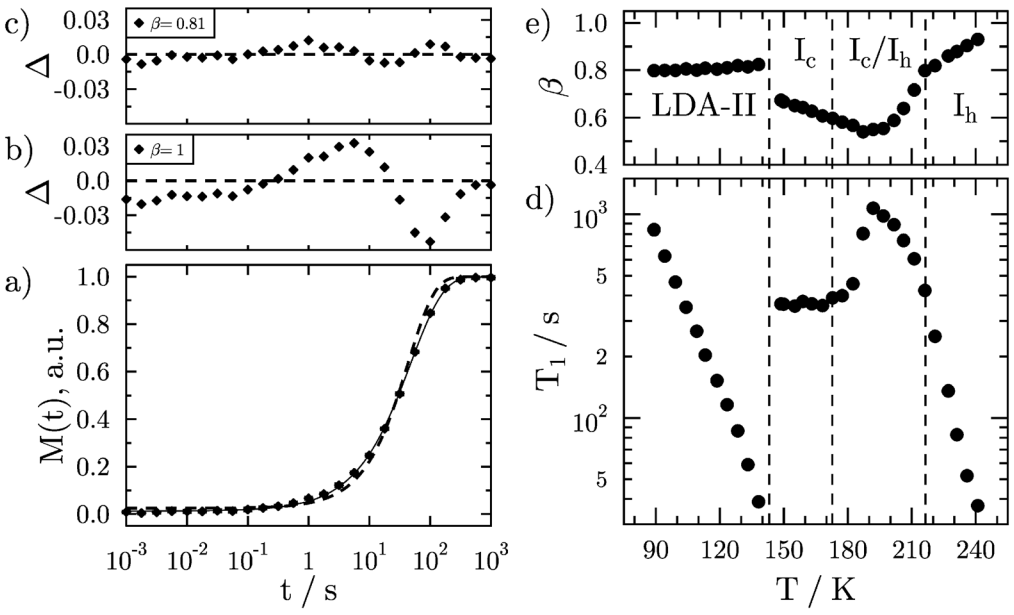

Fig. 2 (a) Normalized relaxation curve $M(t)$ at 134.2 K covering six orders of magnitude in time. The dashed line represents a mono-exponential parametrization ($\beta = 1$) and the stretched-exponential fit (solid line) corresponds to $\beta = 0.81 \pm 0.01$ and $T_1 = (48.3 \pm 0.9)$ s. The residue plots show the deviation $\Delta = M(t)_{exp} - M(t)_{fit}$ between experimental data and fit for a mono-exponential (b) and a stretched-exponential (c) parametrization. T_1 (d) and β (e) of a complete LDA-II transition sequence ending in hexagonal ice I_h.

Both fit parameters, T_1 as well as β, are suitable to monitor changes in the sample state. Their temperature dependence is shown in Fig. 2d and e for a complete LDA-II transition sequence (LDA-II → I_c → I_c/I_h → I_h) finally ending in hexagonal ice.

In this sequence one can clearly discriminate between three domains: below ≈140 K T_1 and β are characteristic of LDA-II.[20] Above 144 K the relaxation parameters indicate that LDA-II has transformed to crystalline cubic ice I_c. It is noteworthy that over quite a wide temperature range between 144 K and ≈175 K T_1 does not change but β does. Between 180 K and 215 K the relaxation parameters gradually approach those found in hexagonal ice I_h. This substantiates the hypothesis of gradual formation of hexagonal ice in a cubic ice matrix.[32–35] Finally, above 215 K, T_1 and β are in agreement with relaxation parameters of ice I_h.[36] However, these findings – highly interesting for the study of crystalline ice phases themselves – are beyond the scope of this paper.

3.2 Gradual crystallization

A second observation, most important for the study of the LDA-II phase, is the failure of the stretched-exponential fits starting at temperatures slightly below the LDA-II → I_c transition (Fig. 3a and the residue plot in Fig. 3b). Obviously, the magnetization recovery becomes bimodal and, indeed, fitting with a superposition of two stretched-exponentials (dashed and dotted lines in Fig. 3a, the residue plot in Fig. 3c) turns out to be a suitable parametrization:

$$M(t) = M_0\left(1 - M_{\mathrm{LDA}}\exp\left[-\left(\frac{t}{T_1^{\mathrm{LDA}}}\right)^{\beta_{\mathrm{LDA}}}\right] - M_{\mathrm{I_c}}\exp\left[-\left(\frac{t}{T_1^{\mathrm{I_c}}}\right)^{\beta_{\mathrm{I_c}}}\right]\right). \quad (5)$$

The occurrence of bimodality is irreversible in the sense that when decreasing the temperature again, the LDA-II magnetization recovery curves stay bimodal. This suggests, without doubt, that the onset of crystallization contaminates the LDA-II phase with traces of ice I_c. These traces are frozen in and do not vanish when the temperature is lowered.

Fig. 4 is a test of this hypothesis. The bimodal fits provide the amplitudes, *i.e.*, the relative amounts of both contributions. The fraction of cubic ice plotted *versus* the consecutive number of the measurement (Fig. 4a) and compared to the temperatures of the measurements (Fig. 4b) clearly demonstrates the growth of cubic crystallites at higher temperatures and their conservation at lower temperatures.§ This gradually growing contamination with ice I_c will be crucial for the analysis of the stimulated echo experiments. However, with the alternating sequence of T_1 and stimulated echo experiments we do have all the tools necessary for a precise correction of these effects.

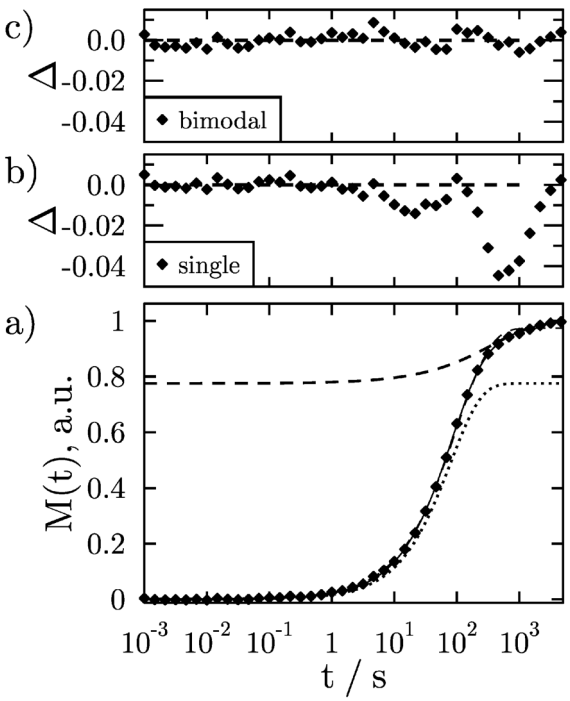

Fig. 3 (a) Magnetization recovery curve at 137.5 K and the best bimodal stretched-exponential fit (black solid line) that is composed by one component associated to LDA-II (dotted line) and another to cubic crystalline ice (dashed line). The residue plots show the deviation $\Delta = M(t)_{\mathrm{exp}} - M(t)_{\mathrm{fit}}$ between the experimental data and the fit for a stretched-exponential (b) and bimodal (c) parametrization.

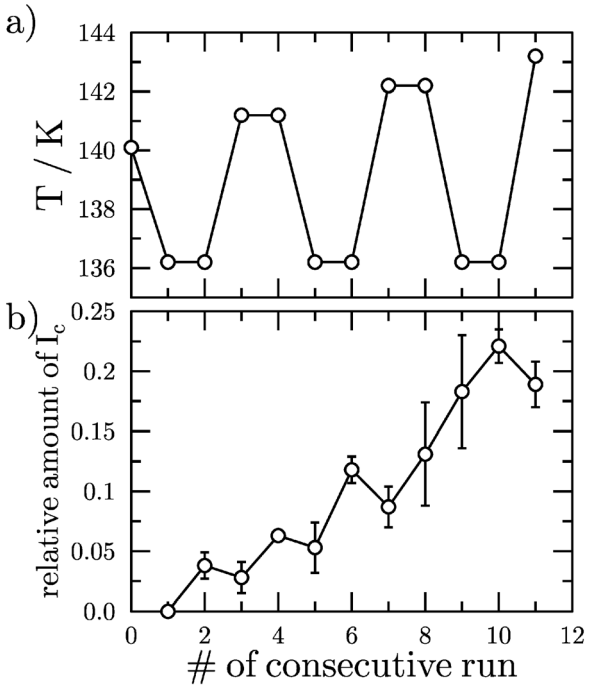

Fig. 4 (a) Chronology of temperature settings in subsequent experiments. (b) Relative amount of cubic ice I_c as deduced from magnetization decay curves.

§ This observation does not contradict statements of our previous publication[20] where we had measured T_1 by more rapid T scans such that crystallization had usually not occured before the next T step.

3.3 Molecular reorientation dynamics

The central experiment of this investigation is the stimulated echo experiment which gives direct access to molecular reorientation times. All stimulated echo decay curves have been measured at a fixed evolution time τ = 7 μs (mid-pulse to mid-pulse). A typical decay of the stimulated echo amplitude is presented in Fig. 5. Obviously, the stimulated echo decay is not much faster than the T_1 relaxation, and both time scales have to be separated by a procedure as indicated at the end of Section 2.1. That is, the experimental data are divided by the interpolated magnetization loss obtained from the independent T_1 measurements. Therefore the remaining decay is given by molecular reorientation exclusively. A fit with eqn (4) now yields three parameters, the final state, S_∞, the correlation time, τ_c, and the stretching parameter, γ. γ is found to be essentially temperature independent, its value of 0.72 ± 0.07 is similar to the values expected from other molecular glass formers.

At this point we are faced with the crucial question: is the stimulated echo decay connected with the glass–liquid transition α-process? This would be the case if the stimulated echo decay time τ_c can be identified with the structural relaxation time τ_α.

Several prerequisites have to be fullfilled in order to substantiate this conjecture.

(i) The final state of the stimulated echo decay *must* be non-zero if the stimulated echo decay originates from molecular reorientation. Its values are unequivocally determined by the geometry of reorientation, *e.g.*, $S_\infty(7\ \mu s) \approx 0.25$ for tetrahedral jumps (as found in crystalline ice I_h[36]), or $S_\infty(7\ \mu s) \approx 0.1$ for fully isotropic reorientation (which one could expect in glasses).

(ii) As indicated in Fig. 1, in the vicinity of T_g the α-process time scale crosses the T_1 curve. Thus, the stimulated echo decay time $\tau_c(T)$ must necessarily decouple from $T_1(T)$.

(iii) At T_g τ_α should be in the order of 100 seconds and τ_c must not be too far away from this value. Furthermore, the temperature dependence of τ_c must result in a "reasonable" glass typical activation energy.

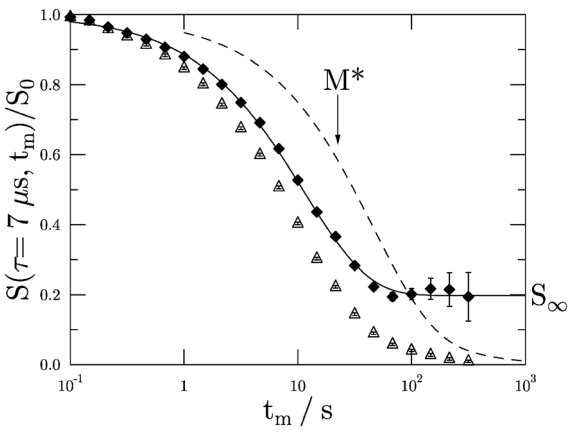

Fig. 5 Typical decay curve of the stimulated echo amplitude in LDA-II: the sampled data (open triangles) has been divided by the effective magnetization $M^*(t_m)$ (dashed line[28]) to obtain the stimulated echo decay (full diamonds) which is then fitted by eqn (4) (solid line).

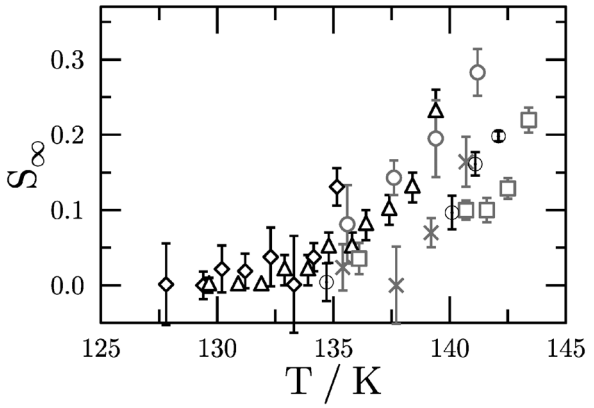

Fig. 6 Final states $S_\infty(\tau = 7\ \mu s)$ as a function of temperature for various samples (indicated by different symbols).

Let us start with item (i), by inspecting the final states. In Fig. 6 $S_\infty(\tau = 7\ \mu s)$ is plotted as a function of temperature. The figure clearly shows that at temperatures above ≈135 K S_∞ is non-zero. However, due to the large scatter of the data (data of several samples are included) one cannot decide between the two reorientation scenarios mentioned above. In other words with S_∞ one cannot distinguish between crystal- and glass-like dynamics. The scatter as well as the temperature dependence in the S_∞ data originate from the data analysis procedure, see below. The vanishing separation in the time scales of τ_c and T_1 at lower temperatures prevents a stable determination of S_∞. The data become more reliable at higher temperatures.

Fig. 7 deals with item (ii), the separation of time scales. A small but highly significant decoupling between τ_c and T_1 with increasing temperature is obvious. But here again, the lacking time scale separation prevents a trustworthy analysis of the correlation times below ≈135 K. The ratio between τ_c and T_1 plotted in Fig. 7b decreases to values down to 0.1 – a clear indication that T_1 even at the highest temperatures before crystallization is not $T_{1,\alpha}$, *cf.* Fig. 1.

Item (iii) can be discussed in the context of Fig. 8 which shows an Arrhenius plot of the reorientational correlation times, τ_c. Due to the merging of the T_1- and τ_c-time scales at lower temperatures, this plot is now restricted to the temperature range above 133 K. Again, this plot contains data from several samples indicated by different symbols. An Arrhenius type T-dependence, *i.e.*, $\tau_c \propto \exp(E_A/kT)$, with $E_A = (22.4 \pm 2)$ kJ mol^{-1} is obtained in this temperature range. The activation energy is of the order of the bond strength of hydrogen bonds; it corresponds to values observed in the Bjerrum defect dynamics in crystalline ice I_h.[36]

If we adopt the technical definition of a glass–liquid transition temperature being that temperature where τ_α becomes 100 seconds, we can extrapolate the straight line in Fig. 8 to see that τ_c arrives at this value at T = 126 K. This value, located deep in the stability range of LDA-II, is significantly smaller than T_g values discussed in the context of calorimetric measurements with a heating rate of 10 K min^{-1} on both LDA-I and LDA-II ices.[6] But it is very close to the T_g of 124 K obtained by

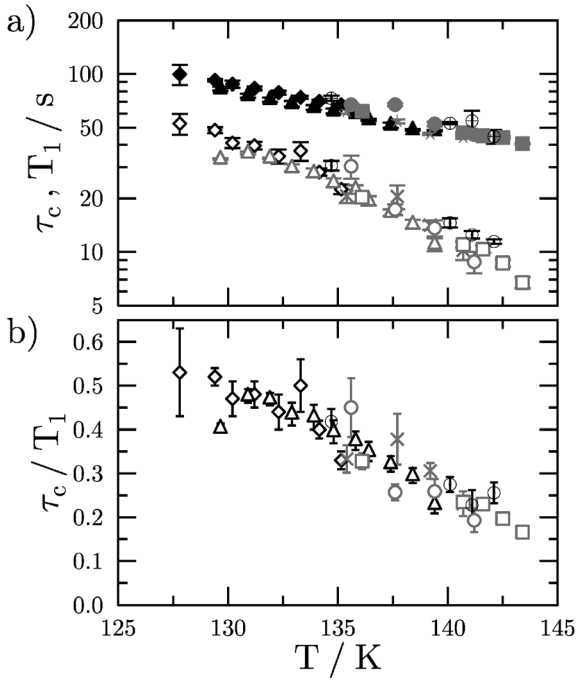

Fig. 7 (a) Temperature dependence of T_1 and τ_c. (b) Ratio of time constants τ_c and T_1 as a function of temperature for various samples (indicated by different symbols).

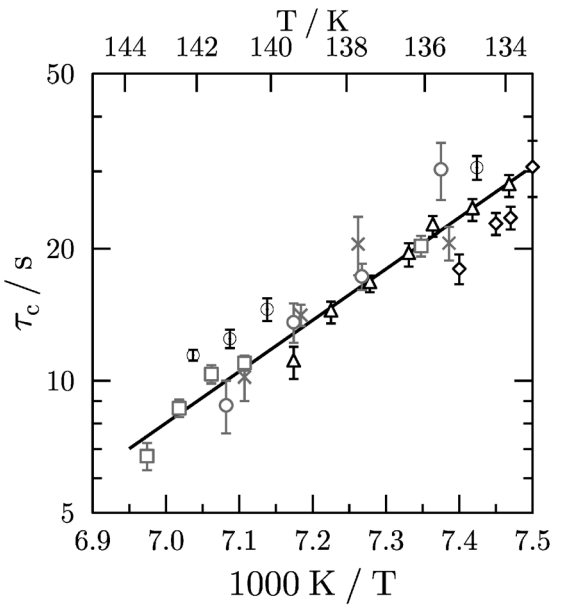

Fig. 8 τ_c as a function of inverse temperature. The slope (black line) of this logarithmic $\tau_c(1/T)$ representation indicates an activation energy of (22.4 ± 2) kJ mol^{-1}.

Handa and Klug for LDA-I samples at a heating rate of 10 K h^{-1} using Tian–Calvet calorimetry.[18]

4 Conclusions

The presented stimulated echo experiments unravel the presence of an ultra-slow reorientation dynamics in LDA-II in the vicinity of the postulated glass–liquid transition temperature. We find time scales in the order of several ten seconds which are of the order of those expected for glass forming liquids. Is this reorientation dynamics the α-relaxation of a supercooled liquid? Or in short, is $\tau_c = \tau_\alpha$? For this, we have formulated three criteria which have to be fullfilled.

Essentially, all our experimental results seem to support the view that τ_c can be identified with τ_α. Our dynamic process takes place on a reasonable time scale, has a rational activation energy and the final states of the correlations function are finite. Furthermore, the short T_1 relaxation times agree with those found in other glasses and differ from the huge values found in crystalline ice phases. In this picture, LDA-II can be imagined as a gradually softening glass.

But do our findings really exclude other, maybe nano-crystalline scenarios? At this point we have to concede that they do not. Even if our final states are finite, they do not rule out a crystalline tetrahedral reorientation. This is because this experiment principally cannot answer the question whether the observed reorientational motion is accompanied or not by translational motion (diffusion) as expected in an ultraviscous liquid. Also, the measured activation energy, compatible with hydrogen bond breaking, is identical to that found in crystalline ices.

In summary, the outcome of these investigations provides strong but not unambiguous arguments supporting the view that LDA-II is a homogeneous glassy state of water.

Acknowledgements

Two of us (K.A.-W. and T.L.) are grateful for financial support from the Austrian Science Fund (Firnberg award T463 and START award Y391) and the European Research Council (ERC Starting Grant SULIWA).

References

1 O. Mishima, L. D. Calvert and E. Whalley, *Nature*, 1984, **314**, 376.
2 G. Johari, *J. Phys. Chem. B*, 1998, **102**, 4711–4714.
3 R. S. Smith and B. D. Kay, *Nature*, 1999, **398**, 788.
4 O. Mishima and Y. Suzuki, *J. Chem. Phys.*, 2001, **115**, 4199.
5 O. Mishima, *J. Chem. Phys.*, 2004, **121**, 3161.
6 M. S. Elsaesser, K. Winkel, E. Mayer and T. Loerting, *Phys. Chem. Chem. Phys.*, 2010, **12**, 708.
7 M. Seidl, M. S. Elsaesser, K. Winkel, G. Zifferer, E. Mayer and T. Loerting, *Phys. Rev. B: Condens. Matter Mater. Phys.*, 2011, **83**, 100201.
8 O. Andersson, *Proc. Natl. Acad. Sci. U. S. A.*, 2011, **108**, 11013–11016.
9 J. S. Tse, D. D. Klug, C. A. Tulk, I. Swainson, E. C. Svensson, C.-K. Loong, V. Shpakov, V. R. Belosludov, R. V. Belosludov and Y. Kawazoe, *Nature*, 1999, **400**, 647.
10 J. S. Tse, D. D. Klug, C. A. Tulk, E. C. Svensson, I. Swainson, V. P. Shpakov and V. R. Belosludov, *Phys. Rev. Lett.*, 2000, **85**, 3185–3188.

11 H. Schober, M. M. Koza, A. Tolle, C. Masciovecchio, F. Sette and F. Fujara, *Phys. Rev. Lett.*, 2000, **85**, 4100–4103.
12 O. Andersson and H. Suga, *Phys. Rev. B: Condens. Matter Mater. Phys.*, 2002, **65**, 140201.
13 M. M. Koza, H. Schober, B. Geil, M. Lorenzen and H. Requardt, *Phys. Rev. B: Condens. Matter Mater. Phys.*, 2004, **69**, 024204.
14 O. Mishima and H. Stanley, *Nature*, 1998, **396**, 329–335.
15 P. H. Poole, F. Sciortino, U. Essmann and H. E. Stanley, *Nature*, 1992, **360**, 324–328.
16 R. J. Nelmes, J. S. Loveday, T. Strassle, C. L. Bull, M. Guthrie, G. Hamel and S. Klotz, *Nature*, 2006, **2**, 414.
17 K. Winkel, D. T. Bowron, T. Loerting, E. Mayer and J. L. Finney, *J. Chem. Phys.*, 2009, **130**, 204502.
18 Y. P. Handa and D. D. Klug, *J. Phys. Chem.*, 1988, **92**, 3323–3325.
19 K. Amann-Winkel, F. Löw, P. H. Handle, W. Knoll, J. Peters, B. Geil, F. Fujara and T. Loerting, *Phys. Chem. Chem. Phys.*, 2012, **14**, 16386–16391.
20 F. Löw, K. Amann-Winkel, B. Geil, T. Loerting, C. Wittich and F. Fujara, *Phys. Chem. Chem. Phys.*, 2013, **15**, 576–580.
21 T. Dries, F. Fujara, M. Kiebel, E. Rössler and H. Sillescu, *J. Chem. Phys.*, 1988, **88**, 2139–2147.
22 W. Schnauss, F. Fujara and H. Sillescu, *J. Chem. Phys.*, 1992, **97**, 1378–1389.
23 K. Schmidt-Rohr and H. W. Spiess, *Multidimensional Solid-State NMR and Polymers*, Academic Press, 1994.
24 J. A. Ripmeester, C. I. Ratcliffe and D. D. Klug, *J. Chem. Phys.*, 1992, **96**, 8503.
25 G. Fleischer and F. Fujara, in *NMR – Basic Principles and Progress*, ed. P. Diehl, E. Fluck, H. Gnther, R. Kosfeld and J. Seeling, Springer, Berlin, 1994, vol. 30, pp. 159–207.
26 H. W. Spiess, *J. Chem. Phys.*, 1980, **72**, 6755.
27 F. Fujara, S. Wefing and H. Spiess, *J. Chem. Phys.*, 1986, **84**, 4579–4584.
28 B. Geil, G. Diezemann and R. Böhmer, *Phys. Rev. E: Stat., Nonlinear, Soft Matter Phys.*, 2006, **74**, 041504.
29 K. Winkel, M. Elsaesser, E. Mayer and T. Loerting, *J. Chem. Phys.*, 2008, **128**, 044510.
30 M. Scheuermann, B. Geil, F. Löw and F. Fujara, *J. Chem. Phys.*, 2009, **130**, 024506.
31 M. Scheuermann, B. Geil, K. Winkel and F. Fujara, *J. Chem. Phys.*, 2006, **124**, 224503.
32 Y. P. Handa, O. Mishima and E. Whalley, *J. Chem. Phys.*, 1986, **84**, 2766.
33 W. F. Kuhs, D. V. Bliss and J. L. Finney, *J. Phys., Colloq.*, 1987, **48**, 631–636.
34 A. Elarby-Aouizerat, J. F. Jal, J. Dupuy, H. Schildberg and P. Chieux, *J. Phys., Colloq.*, 1987, **48**, 465–470.
35 T. C. Hansen, M. M. Koza, P. Lindner and W. F. Kuhs, *J. Phys.: Condens. Matter*, 2008, **20**, 285105.
36 B. Geil, T. M. Kirschgen and F. Fujara, *Phys. Rev. B: Condens. Matter Mater. Phys.*, 2005, **72**, 014304.

